DOI: 10.1002/chem.200501566

A QM/MM Study of Cisplatin–DNA Oligonucleotides: From Simple Models to Realistic Systems

Arturo Robertazzi and James A. Platts*[a]

Abstract: QM/MM calculations were employed to investigate the role of hydrogen bonding and π stacking in several single- and double-stranded cisplatin–DNA structures. Computed geometrical parameters reproduce experimental structures of cisplatin and its complex with guanine–phosphate–guanine. Following QM/MM optimisation, single-point DFT calculations allowed estimation of intermolecular forces through atoms in molecules (AIM) analysis. Binding energies of platinated single-strand DNA qualitatively agree with myriad experimental and theoretical studies showing that complexes of guanine are stronger than those of adenine. The topology of all studied complexes confirms that platination strongly affects the stability of both single- and double-stranded DNAs: Pt–N–H···X (X = N or O) interactions are ubiquitous in these complexes and account for over 70% of all H-bonding interactions. The π stacking is greatly reduced by both mono- and bifunctional complexation: the former causes a loss of about 3–4 kcal mol^{-1}, whereas the latter leads to more drastic disruption. The effect of platination on Watson–Crick GC is similar to that found in previous studies: major redistribution of energy occurs, but the overall stability is barely affected. The BH&H/AMBER/AIM approach was also used to study platination of a double-stranded DNA octamer d(CCTG*G*TCC)·d(GGACCAGG), for which an experimental structure is available. Comparison between theory and experiment is satisfactory, and also reproduces previous DFT-based studies of analogous structures. The effect of platination is similar to that seen in model systems, although the effect on GC pairing was more pronounced. These calculations also reveal weaker, secondary interactions of the form Pt···O and Pt···N, detected in several single- and double-stranded DNA.

Keywords: density functional calculations · hydrogen bonds · oligonucleotides · platinum · stacking interactions

Introduction

cis-Diamminodichloroplatinum(II) (*cis*-$[PtCl_2(NH_3)_2]$, cisplatin, or *cis*-DDP) is one of the most widely used anticancer drugs and is particularly active in treating several different tumours.[1,2] Despite its high activity, cisplatin has some critical drawbacks such as severe toxic side effects, inherent and acquired resistance, and limited solubility in aqueous solution.[3] Research into new platinum drugs is therefore intense, with improved efficiency and reduced toxicity the main aims. Many platinum(II) complexes have been synthesized and tested as potential drugs, including numerous direct analogues of the general form *cis*-$[PtX_2A_2]$ as well as platinum(IV) compounds,[4] and other "rule breakers".[3] However, only three more platinum drugs have been registered for clinical use, namely, oxaliplatin,[5] carboplatin,[6,7] and nedaplatin.[8] The mechanism of anticancer action is well-studied,[3,9–22] and DNA was identified as the main target: after activation via hydrolysis,[23,24] cisplatin forms bifunctional inter- and intrastrand cross-link complexes, triggering structural changes and preventing DNA transcription activity and/or inducing recognition by damage-repair proteins,[25] ultimately resulting in cell death through apoptosis, necrosis or both.[26]

In recent years, theoretical approaches have increasingly added insight into cisplatin's chemistry, including its electronic structure,[27,28] hydrolysis,[27,29–31] structural properties of DNA base–cisplatin complexes[27,32,33] and effect on DNA base pairing.[34–36] For instance, Eriksson et al.[37] studied the attack of activated cisplatin on DNA and showed that guanine gives a lower barrier than adenine for both mono- and bifunctional complexes. Leszczynski et al.[32] showed that the expected G-Pt-G structure is indeed the most stable, along with A-Pt-G. They also studied the effect of sugar-phosphate

[a] A. Robertazzi, Dr. J. A. Platts
School of Chemistry, Cardiff University
Park Place, Cardiff CF10 3AT (UK)
Fax: (+44) 2920-874-030
E-mail: platts@cardiff.ac.uk

conformation on *cis*-$[Pt(NH_3)_2\{1,2\text{-d(BpB)}\}]^{2+}$ (B = guanine or adenine)[38] and found excellent agreement between B3LYP and experimental structures. Carloni et al.[39] used Car–Parrinello molecular dynamics (MD) to investigate DNA–cisplatin interactions, and found close agreement between DFT and experiment, for example, in thermodynamic aspects of cisplatin hydrolysis. Other studies suggest that although severely distorted, the hydrogen-bond pattern in the GC pair is essentially retained upon platination.[34–36]

Recently, we used DFT and atoms in molecules (AIM) analysis to characterise the role of hydrogen bonding and other intermolecular interactions in these processes.[40,41] Here we continue to develop this approach, studying both single- and double-stranded di- and trinucleotides by hybrid QM/MM calculations: the QM area was treated with the BH&H[42] functional, which has been recently shown to reproduce well the π-stacking geometries and energies of more conventional post-HF methods. After establishing the validity of this approach using small model systems, we go on to examine platination of DNA duplexes, both in isolation and within a model of octameric double helix, previously studied by NMR methods.[43]

Computational Details

All DFT calculations were performed with the Gaussian 03 suite of programs.[44] Throughout this work, we made extensive use of Becke's "half-and-half" functional, BH&H,[42] as we have recently shown that this functional, with polarised and diffuse basis sets, is able to reproduce results of post-HF methods for several archetypal π-stacked complexes.[45] In this work, the success of the BH&H functional is attributed to cancellation of errors between Hartree–Fock (HF) and LDA exchange energies: nonetheless, it performed remarkably well in all cases tested. Comparison against literature CCSD(T) binding energies for 10 complexes and MP2 values for 22 complexes, including stacked dimers of substituted benzenes and pyridines and DNA bases, yielded average errors of less than 0.5 kcal mol^{-1} and a maximum error of less than 1 kcal mol^{-1}. However, despite this excellent performance for π stacking, it was found that BH&H significantly overestimates the strength of the hydrogen bonds in Watson–Crick GC and AT pairs, in common with many hybrid DFT methods. For larger complexes, the ONIOM method[46–50] was used to split the system into QM and MM regions, with nucleobases entirely within the high-level layer, that is, BH&H/6-311++G(d,p) (for the Pt atom the SDD[51] basis set and ECP was used), and sugar–phosphate backbone treated using AMBER potentials.[52] To determine the wavefunction and carry out AIM analysis, subsequent single-point calculations on the entire structure were performed using BH&H/6-311++G(d,p).

To quantify intermolecular interactions, as in our previous studies,[40,45] topological analysis of computed electron densities ρ was performed using the AIM2000 package.,[53,54,55] This is based upon those critical points (CPs) where the gradient of the density $\nabla\rho$ vanishes. Such points are classified by the curvature of the electron density, for example, bond or (3,−1) CPs have one positive curvature (in the internuclear direction) and two negative curvatures (perpendicular to the bond). Properties evaluated at such BCPs characterise the bonding interactions present,[56] and have been widely used to study intermolecular interactions. Many studies have demonstrated approximately linear relations between H-bond stabilisation energy and both the increase in density at H···B BCP and the decrease at A−H for a wide range of A−H···B systems.[57,58] For instance, we recently set out an AIM-based method for quantifying π-stacking interactions,[45] in which the electron density collected between interacting molecules $\Sigma\rho_\pi$ accurately describes the π-stacking energy. In all cases, the energy from electron density properties corresponds to the BSSE-corrected energy.[59] To check the effect of including the MM region in single DFT calculations, we also performed single-point calculations on structures without the sugar-phosphate backbone, which was replaced by H atoms: in all cases considered, identical topologies (i.e., number and type of CPs) and almost identical electron densities (differences less than 0.0005 a.u.) were found.

Results and Discussion

Having established that the hybrid BH&H density functional can account for π-stacking interactions in model systems of DNA,[45] it is important to test its performance for cisplatin and related structures before using it to analyse the effects of platination on π stacking. The optimised structure of cisplatin obtained at the BH&H/6-311++G(d,p)(SDD) level is reported in Table 1, along with experimental and various theoretical values. In general, agreement is excellent with both experimental values from solvent-free crystal[60] and those from HF,[29] MP2,[29] and DFT,[61] with bond lengths within about 0.05 Å of experimental and similar bond angles to all previous theoretical estimates.

Table 1. Bond lengths and angles of cisplatin.

	BH&H	HF/6-31 G(d,p)[a]	MP2/6-31 G(d)[a]	BLYP[b]	Exptl[c]
Pt–N [Å]	2.058	2.139	2.090	2.065	2.01 ± 0.04
Pt–Cl [Å]	2.283	2.348	2.312	2.315	2.33 ± 0.01
N-Pt–N [°]	97.9	95.0	96.5	98.0	
N-Pt-Cl [°]	83.4	84.7	84.9	83.0	
Cl-Pt-Cl [°]	95.2	95.6	93.8	95.5	

[a] Hausheer et al.[29] [b] Carloni et al.[61] [c] In the solvent-free crystal.[60]

In addition, comparison between optimised and X-ray[62] data for *cis*-$[Pt(NH_3)_2\{d(pGpG)\}]$, where p indicates the sugar-phosphate backbone of DNA, is excellent (see Table 2). The reported crystal structure contains four independent molecules in the unit cell, with estimated errors of about 0.02 Å and 0.5°, and significant variation between each molecule. Within these variations, calculated values are close to experimental data: typically the discrepancy in Pt–

Table 2. Geometric features of *cis*-$[Pt(NH_3)_2\{d(pGpG)\}]$.[a]

	BH&H	Exptl[b]
Pt–N1 [Å]	2.030	2.050(0.036)
Pt–N2 [Å]	2.032	2.055(0.045)
Pt–N7A [Å]	2.032	1.968(0.055)
Pt–N7B [Å]	2.031	2.015(0.063)
N7A-Pt-N1 [°]	88.5	89.6(1.3)
N7A-Pt-N2 [°]	177.0	176.8(2.5)
N7A-Pt-N7B [°]	91.0	88.3(2.2)
N1-Pt-N2 [°]	92.2	91.7(1.0)
N1-Pt-N7B [°]	176.7	175.9(2.5)
N2-Pt-N7B [°]	88.2	90.3(1.8)
Gua/Gua[c] [°]	78.0	81.2(4.3)

[a] See Figure 1a for labelling. [b] Average over four molecules reported by Sherman et al.[62] sd in parentheses. [c] Dihedral angle between guanine residues: see Orbell et al.[63] and Figure 1b.

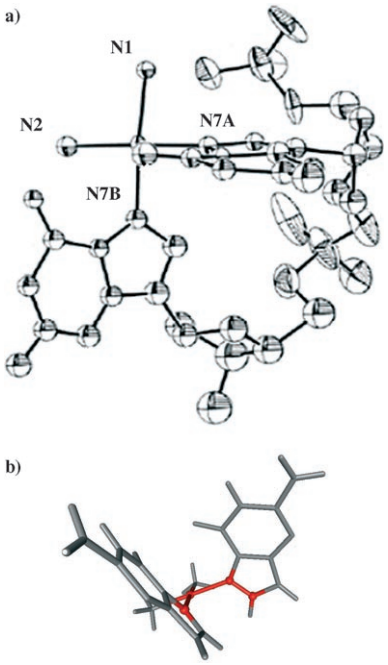

Figure 1. a) Atom labelling in *cis*-[Pt(NH$_3$)$_2$\{d(pGpG)\}],[62] and b) dihedral angles between guanine bases, in accord with Orbell's convention.[63]

N bonds is around 0.02 Å, and in bond and dihedral angles about 1–2°.

Table 3 reports binding energies for all studied mono- and bifunctional complexes of cisplatin with single-stranded DNA, along with bond lengths and electron densities of platinum···base bonds (Pt–X, where X = N or O). As expected from many previous studies,[32,64–66] guanine complexes are more stable than adenine complexes. For instance, cisGpG$_{mono}$ has the highest binding energy of all monofunctional complexes, with cisplatin directly bound to the nitrogen atom of one guanine residue. cisGpA$_{mono}$, in which the guanine molecule not directly bound to the metal centre is substituted with adenine, has a binding energy

Table 3. Binding energies (BE) and bonding properties of platinated adducts.

	BE [kcal mol^{-1}]		r(Pt–X) [Å]	ρ_c(Pt–X) [a.u.]
cisGpG$_{mono}$	147.17	Pt–N$_G$	2.022	0.119
cisGpA$_{mono}$	143.45	Pt–N$_G$	2.011	0.123
		Pt···N$_A$	3.421	0.009
cisApG$_{mono}$	127.51	Pt–N$_A$	2.100	0.113
cisGpGpG$_{mono}$	174.40	Pt–N$_G$	2.014	0.120
		Pt···N$_G$	3.149	0.014
cisGpG$_{bi}$	312.43	Pt–N$_G$	2.032	0.116
		Pt–N$_G$	2.032	0.117
cisGpA$_{bi}$	285.22	Pt–N$_G$	2.017	0.122
		Pt–N$_A$	2.012	0.124
cisGpG$_{chel}$	284.57	Pt–N$_G$	2.049	0.109
		Pt-O$_G$	2.111	0.084
cisGpGpG$_{bi}$	397.96	Pt–N$_G$	2.043	0.112
		Pt–N$_G$	2.009	0.123
cisGpApG$_{bi}$	396.35	Pt–N$_G$	2.029	0.117
		Pt–N$_A$	2.004	0.126

4 kcal mol^{-1} lower, as well as a slightly shorter, stronger Pt–X bond (r = 2.011 Å, ρ_c = 0.123 a.u.). Interestingly, AIM reveals a weak secondary interaction between Pt and N7 of adenine, with ρ_c = 0.009 a.u. (see below). The binding energy for cisGpGpG$_{mono}$ (see Figure 2) is much larger than for the

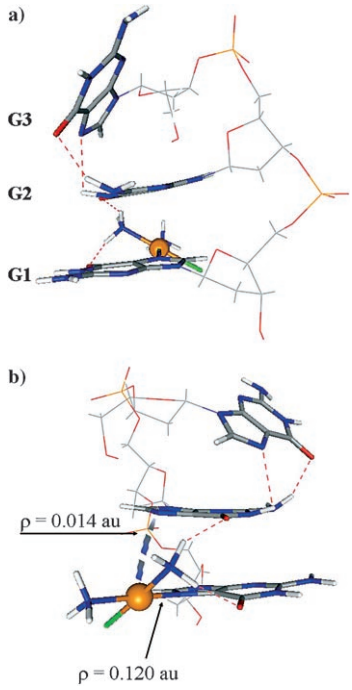

Figure 2. Optimised geometry of cisGpGpG$_{mono}$ showing a) distortion of G···G interaction and b) electron densities at the P–-N$_G$ bond and Pt···N secondary interaction.

dinucleotides, approximately 30 kcal mol^{-1} more than for cisGpG$_{mono}$. However, the Pt–N$_G$ bond is similar in distance and density to those of platinated dinucleotides, and this suggests that the extra binding energy may be mostly due to electrostatic attraction between phosphate and platinum. As above, AIM reveals a secondary interaction to N7 of G2, with ρ_c = 0.014 a.u. (see Figure 2b).

The binding energies of bifunctional adducts are more than twice those of monofunctional complexes, due to the +2 charge on these complexes. The trend observed for monofunctional complexes is preserved, with guanine complexes more strongly bound than adenine complexes. In particular, cisGpG$_{bi}$ is more than 25 kcal mol^{-1} more stable than cisGpA$_{bi}$, a much larger difference than observed in the monofunctional complexes above. The structure in which platinum is chelated by O and N of a single guanine residue has similar stability to cisGpA$_{bi}$, that is, considerably less than the bifunctional adduct, in agreement with previous work.[40,67,68] The trinucleotides show a similar trend, but here the difference in binding energy between cisGpGpG$_{bi}$ and cisGpApG$_{bi}$ is only 2 kcal mol^{-1}. To rationalise these differences, we turn to AIM analysis for decomposition into covalent bonding, H-bonding and π-stacking effects.

Table 4 compares H-bonding and π-stacking energies estimated from AIM data between free and platinated di- and trinucleotides. Clearly, H-bonding is prevalent in platinated species, with strong interactions involving Pt–NH and Pt–Cl

Table 4. H-bonding and π stacking of free and platinated oligonucleotides [kcal mol^{-1}].

	Platinated		Free	
	E_{HB}[a]	E_{π}[a]	E_{HB}[a]	E_{π}[a]
cisGpG$_{mono}$	23.22	5.25	20.00	2.42
cisGpA$_{mono}$	20.83	3.00	9.75	5.90
cisApG$_{mono}$	36.28	2.13	9.75	5.90
cisGpGpG$_{mono}$	25.36	6.97 (3.18+3.79)[b]	20.70	9.70

[a] AIM estimated energy. [b] Contributions from G1···G2 and G2···G3 in parentheses.

groups as donors and acceptors. For instance, in cisGpG$_{mono}$, the energy due to these interactions is 21 kcal mol^{-1}, and only 2 kcal mol^{-1} comes from a single N–H···O H-bond between guanine and phosphate, that is, no interbase H-bonds are detected here, unlike free oligonucleotides, for which such interactions are significant. Similarly, for cisGpA$_{mono}$ the H-bonding energy of Pt ligands is 15 kcal mol^{-1}, less than 5 kcal mol^{-1} of which comes from interbase H-bonding, and for cisApG$_{mono}$, 25 kcal mol^{-1} is due to cisplatin NH_3 ligands. Thus, in these complexes most of the H-bond energy (typically more than 70%) originates from the ammine ligands of cisplatin.

In contrast, platination reduces all π-stacking energies bar one by 3–4 kcal mol^{-1}, accompanied by substantial geometrical distortion (Figures 2 and 3). It appears that strong Pt–N–H···X (X = N, O) H-bonds cause the two purine residues to point towards each other, and this leads to a loss of π-stacking energy. Only in cisGpG$_{mono}$ is π stacking enhanced by platination, from 2.42 to 5.25 kcal mol^{-1}; however, this may be due to the initial strong distortion of the structure of free GpG and the low value of E_{π} in free GpG. In the trinucleotide cisGpGpG$_{mono}$ (Figure 2) both G···G stacks are of approximately equal energy, and sum to about 3 kcal mol^{-1} less than for the free complex.

When cisplatin binds to DNA, it is well known[9] that the major products are 1,2-intrastrand G-Pt-G and A-Pt-G complexes: Table 5 reports H-bonds and π-stacking energies of these bifunctional adducts. cisGpG$_{bi}$ has two almost symmetric Pt–N–H···O interactions with energies of 10 kcal mol^{-1} each (Figure 4a), whereas cisGpA$_{bi}$ (Figure 4b) has just one such interaction with guanine, along with a much weaker Pt–N–H···N contact with adenine. In the guanine chelate complex cisGpG$_{chel}$ (Figure 4c), strong H-bonds between cisplatin ammine ligands and O6/N7 of the uncoordinated guanine residue lead to a high H-bond energy. Therefore, as for monofunctional complexes, most H-bonding energy stems from ammine ligands of cisplatin. In the trinucleotide complexes, H-bonding energy is larger than in the free structure, and again this comes mainly from cisplatin. For instance, in cisGpGpG$_{bi}$ G3 interacts via Pt–N–H···O with cisplatin, while Pt–N–H···O and N–H···N are found between cisplatin

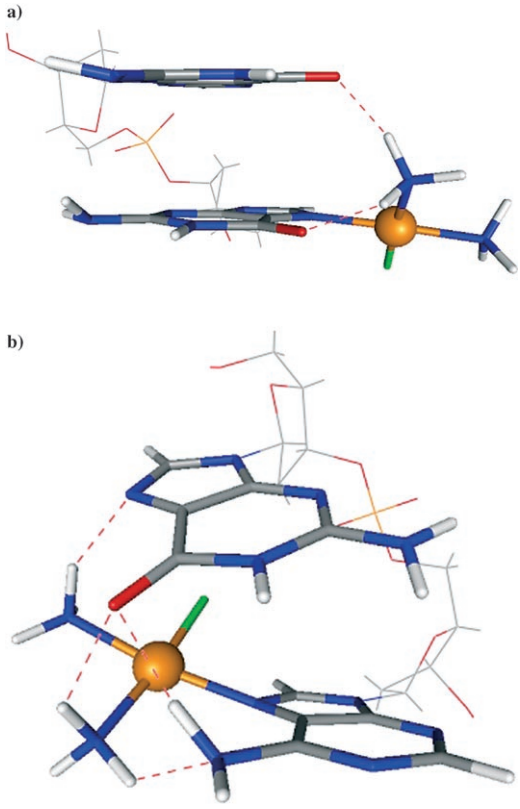

Figure 3. H-bonds in a) cisGpG$_{mono}$ and b) cisApG$_{mono}$.

Table 5. H-bonding and π stacking of free and platinated oligonucleotides [kcal mol^{-1}].

	Platinated		Free	
	E_{HB}[a]	E_{π}[a]	E_{HB}[a]	E_{π}[a]
cisGpG$_{bi}$	21.16	0.00	20.00	2.42
cisGpA$_{bi}$	12.92	1.25	9.75	5.90
cisGpG$_{chel}$	23.88	0.00	20.00	2.42
cisGpGpG$_{bi}$	28.81	5.04 (5.04+0.00)[b]	20.70	9.70
cisGpApG$_{bi}$	26.18	5.94 (5.02+0.92)[b]	17.93	10.40

[a] AIM estimated energy. [b] Contributions from G1···G2 & G2···G3 for cisGpGpG$_{bi}$ and G1···A2 & A2···G3 for cisGpApG$_{bi}$ in parentheses.

and G1 (see Figure 4d). The importance of H-bonding involving cisplatin over that between bases is also apparent in the NH_2 groups of guanine and adenine, which are significantly less pyramidal than in optimisation of free DNA (average sum of angles ca. 350°, cf. 330° in free DNA).

It has been deduced from structural data, both experimental and theoretical, that one of the main effects of platination is to disrupt π stacking between bases.[62,69–74] The topological data in Table 5 support this: in cisGpG$_{bi}$, cisGpG$_{chel}$ and cisGpGpG$_{bi}$ no BCPs corresponding to π stacking are located between the platinated bases, and hence $E_{\pi} = 0$ in all these cases. In complexes involving adenine, that is, cisGpA$_{bi}$ and cisGpApG$_{bi}$, a solitary π-stacking CP between G and A is located, corresponding to an energy

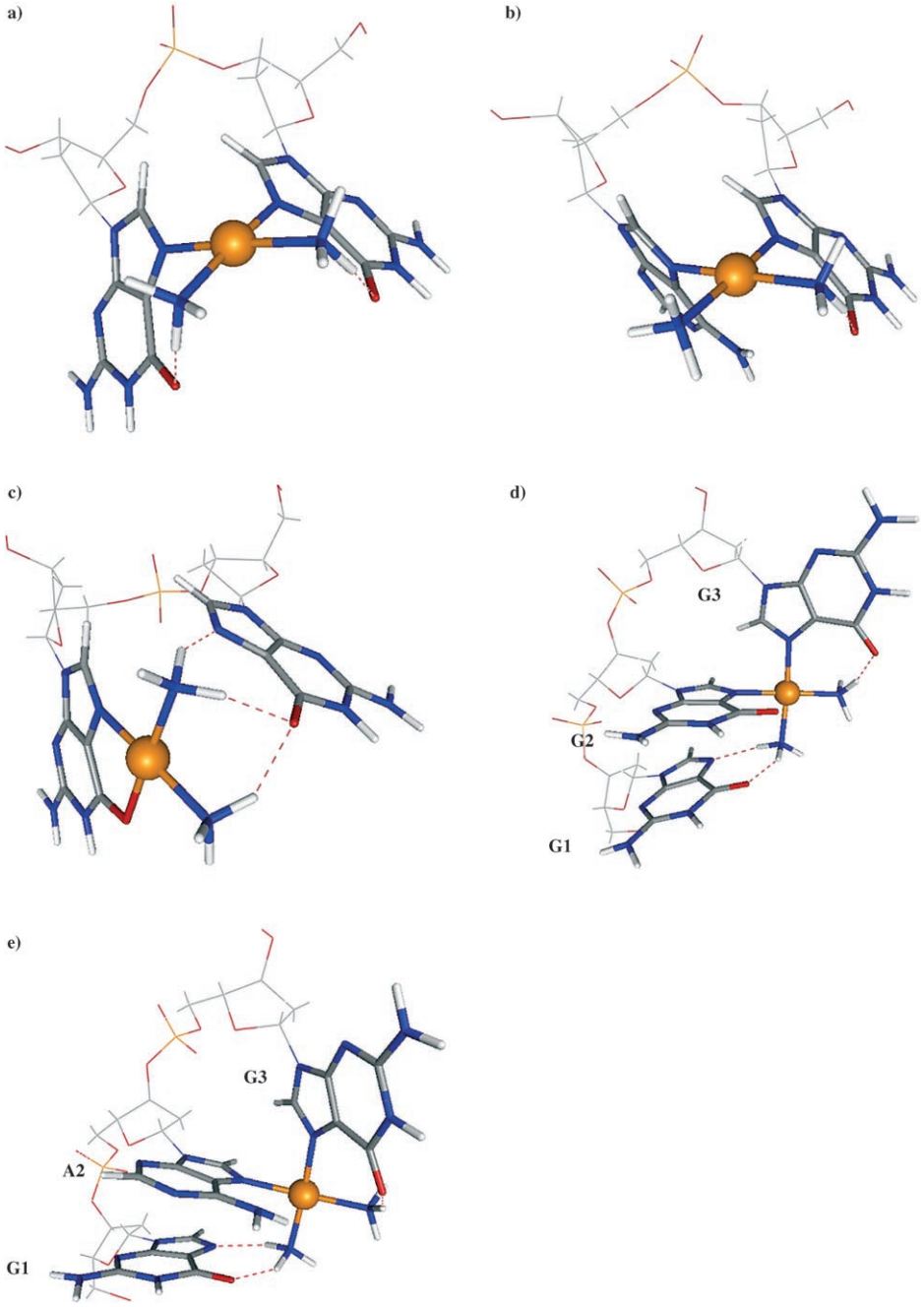

Figure 4. Optimised geometries of a) cisGpG$_{bi}$, b) cisApG$_{bi}$, c) cisGpG$_{chel}$, d) cisGpGpG$_{bi}$ and e) cisGpApG$_{bi}$.

contribution of just 1 kcal mol^{-1}. In the two trinucleotides considered, stacking between the unplatinated base and its neighbour is hardly disrupted from that found in the free structure, that is, 5 kcal mol^{-1} for G···G and 6 kcal mol^{-1} for G···A. In this way, topological analysis by AIM is able to quantify the disruption of intrastrand stacking, showing it to be large in all cases and largest between guanine residues, while interactions between the remaining bases are virtually unchanged.

As well as affecting H-bonding and π stacking within DNA strands, platination can also disrupt interactions between strands. To study this we optimised mono- and bifunctional and chelate GpG·CpC complexes (see Figure 5), denoted cisGpG·CpC$_{mono}$, cisGpG·CpC$_{bi}$ and cisGpG·CpC$_{chel}$, respectively, as well as one bifunctional platinated GpA·CpT (denoted cisGpA·CpT$_{bi}$). Properties of covalent Pt–N(O) bonds follow the patterns outlined above, though as in previous work[40] the presence of cytosine in the base pair leads to a systematic strengthening of these interactions. AIM analysis reveals a number of secondary interactions Pt···X (X = N, O), detailed in Table 6. As in single-stranded complexes, these interactions are weak with bond lengths longer than 3 Å and ρ_c between 0.01 and 0.02 a.u., that is, around 1 Å longer and an order of magnitude weaker than the "direct" interactions. Hydrogen bonds within strands and involving cisplatin are almost identical to those in the single-stranded complexes, and so no further details are reported on these interactions.

Stacking interactions in duplexes can be both intrastrand (S) and interstrand (IS), in addition to the normal Watson–Crick pairing of GC and AT. In free GpG·CpC, these interactions have been estimated at $GG_S = 7.06$, $CC_S = 3.79$ and $GC_{IS} = 2.28$ kcal mol^{-1} (Table 6).[41] These values change only slightly in cisGpG·CpC$_{mono}$, in which GG_S is reduced while CC_S and GC_{IS} are slightly enhanced. The effect of platination is more pronounced for bifunctional and chelating adducts: as expected, cisplatin heavily disrupts π stacking between guanine residues, which is reduced by about 70% from the original value. However, unlike in the single-strand case, stacking energy in these complexes is nonzero, and stacking CPs are found between guanine residues. This appears to be due to a "buffering" effect of the three strong hydrogen bonds to cytosine, which together with CC_S interaction and the constraints of the second strand backbone keep the guanine residues together more

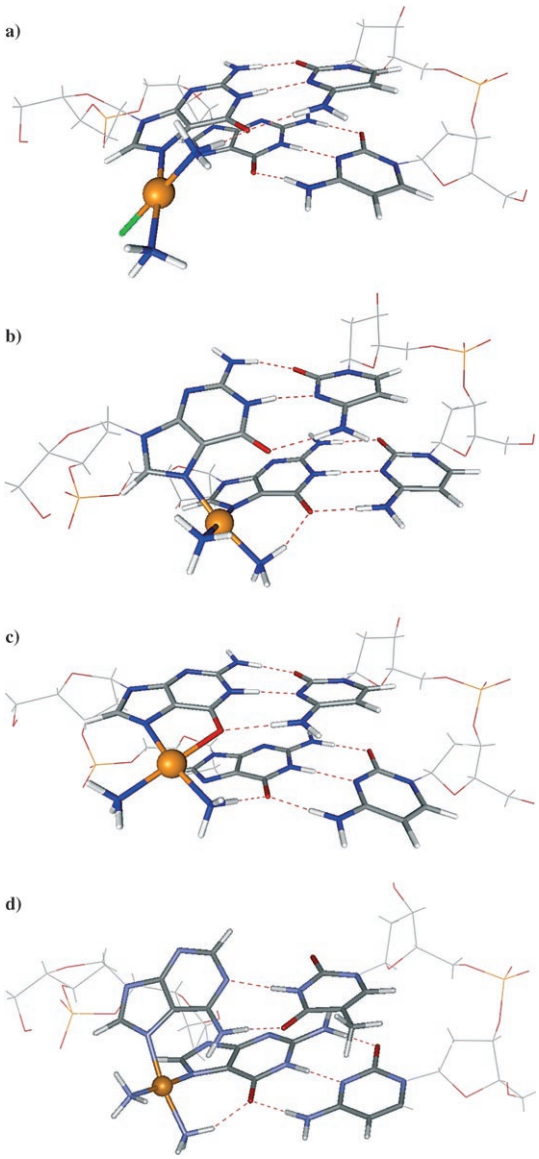

Figure 5. Optimised geometries of a) cisGpG·CpC$_{mono}$, b) cisGpG·CpC$_{bi}$, c) cisGpG·CpC$_{chel}$ and d) cisGpA·CpT$_{bi}$.

Table 6. Interactions in platinated duplexes.

	Pt–X		$E_{N-H\cdots O}$ [kcal mol^{-1}]	E_{π} [kcal mol^{-1}]		
	r [Å]	ρ [a.u.]		GG_S (GA_S)[a]	CC_S (CT_S)[b]	GC_{IS} (CA_{IS}, TG_{IS})[c]
free GpG·CpC	–	–	–	7.06	3.79	2.28
free GpA·CpT	–	–	–	5.22	2.92	2.15
cisGpG·CpC$_{mono}$	2.007	0.124	14.32	6.65	4.60	3.41
cisGpG·CpC$_{bi}$	2.022	0.120	10.82	2.28	3.10	4.31
	2.017	0.122				
	3.026[d]	0.017				
cisGpG·CpC$_{chel}$	2.060	0.107	13.80	2.08	4.97	3.02
	2.080	0.093				
	3.028[d]	0.018				
cisGpA·CpT$_{bi}$[e]	2.008	0.125	8.75	2.15	3.60	2.71
	2.019	0.121				

[a] GG_S or GA_S: purine intrastrand. [b] CC_S or CT_S: pyrimidine intrastrand. [c] GC_{IS} contacts in all GpG·CpC species, CA_{IS} in free GpA·CpT, TG_{IS} in cisGpA·CpT$_{bi}$: interstrand. [d] Pt···O/N secondary interaction. [e] First row refers to Pt–G and second to Pt–A.

Table 7. Electron density [a.u.] of AT and GC pairs in platinated duplexes.

	H4···O6 (H3···N1)	H1···N3 (H6···O4)	H2···O2	$\Sigma\rho_{CP}$
free GC	0.0520	0.0436	0.0365	0.132
free AT	0.0586	0.0285		0.087
cisGpG·CpC$_{mono}$	0.0389[a]	0.0470	0.0506	0.137
	0.0535	0.0418	0.0360	0.131
cisGpG·CpC$_{bi}$	0.0377	0.0540	0.0407	0.132
	0.0351	0.0457	0.0492	0.130
cisGpG·CpC$_{chel}$	0.0260[a]	0.0607	0.0510	0.138
	0.0380	0.0430	0.0457	0.128
cisGpA·CpT$_{bi}$	0.0317	0.0478	0.0519	0.131
	0.0504	0.0387		0.089

[a] For monofunctional and chelate complexes, the first row refers to platinated GC pair.

than in the platinated single-strand complexes (cf. Table 5). Similarly, the GA_S intrastrand stacking energy in cisGpA·CpT$_{bi}$ (Figure 5d) is reduced by about 60%, from 5.22 to 2.15 kcal mol^{-1}, while CT_S is hardly changed. The effect of platination on interstrand interactions is notable: distortion of the duplex disrupts CA_{IS} (ca. 2 kcal mol^{-1})[41] and induces a new contact between T and G (TG_{IS} = 2.71 kcal mol^{-1}).

As well as stacking interactions, platination is known to affect Watson–Crick pairing between G & C and A & T. Table 7 reports the electron density at the H-bond CP for each interaction, which shows that platination weakens H4···O6 but strengthens H1···N3 and H2···O2, such that the overall electron density of the GC pair is hardly changed. This pattern is almost symmetrical in the bifunctional complex cisGpG·CpC$_{bi}$, while in cisGpA·CpT, the H-bond in which adenine acts as a proton donor (H6···O4) is considerably stronger than in free AT, while where adenine is a proton acceptor (H3···N1) the H-bond is weakened. In cisGpG·CpC$_{mono}$, interaction of the unplatinated guanine residue with cytosine is barely affected by the presence of cisplatin, but in cisGpG·CpC$_{chel}$ both GC pairs are affected, to the extent that unplatinated GC is the weakest found in this work.

To demonstrate what we believe to be the potential of the BH&H/AMBER/AIM approach, and to provide a better model of platination of DNA, we report some preliminary calculations on larger scale complexes. Figure 6 shows the QM/MM optimised geometry of a cisplatin adduct of the octamer duplex d(CCTG*G*TCC)·d(GGACCAGG),[43] (platinated guanine residues indicated by *) solvated by about 400 H_2O molecules. As shown in Figure 6, the QM region includes four bases, that is, cisGpG·CpC$_{bi}$ and cisplatin, while the remaining DNA bases, sugar-phosphate backbone and water molecules were treated with AMBER. The experimental NMR structure (PDB entry 1AU5)[43] was used as the starting point for optimisation. The ability of AMBER

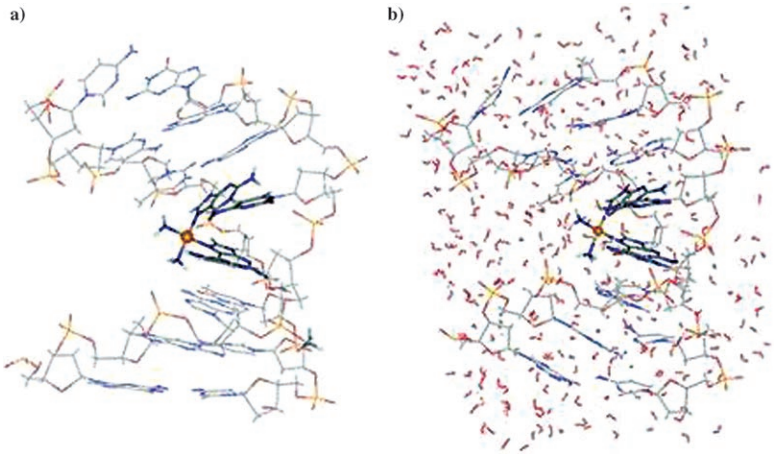

Figure 6. Experimental a) and optimised b) geometries of cisplatin–DNA adduct.

to reproduce DNA structures is well reported,[75] so our focus here is on the QM region.

Table 8 and Figure 7 indicate general agreement between optimised and NMR structures: bond lengths are slightly overestimated in our calculations by between 0.02 and 0.06 Å, while angles deviate by 2–8°. The reproduction of the dihedral angle between guanine residues and its change from the model cisGpG complex (Table 2) supports our choice of an ONIOM:BH&H/AMBER method. The RMS deviation between calculated and optimised Cartesian coordinates is 2.12 Å, which compares reasonably well with the values of 0.7–1.3 Å quoted in ref. [43] for differences between different refinements against NMR data, albeit for the entire octamer duplex structure.

We then evaluated the topology of electron density for both the experimental (cis_{exptl}) and calculated (cis_{QM}) geometries of platinated GpG·CpC within this octamer duplex. As noted above, inclusion of the MM region in these calculations makes essentially no difference in smaller duplexes, so here the QM region was extracted from the overall structure, link atoms replaced with hydrogen and a single-point DFT calculation carried out. Electron density at Pt–N bonds is similar in both structures (0.118 and 0.123 a.u. in calculated structure vs 0.127 and 0.133 a.u. from experimental structure). Moreover, both structures contain secondary Pt···O interactions: two are present in the experimental structure but just one in the optimised geometry. Despite the similarity in geometries noted above, differences in the electron density of intermolecular interactions are more apparent: in the experimental geometry, just two CPs corresponding to π stacking are found, along with the expected three for each GC pair. In contrast, four stacking CPs are found in the optimised geometry, as well as two Pt–N–H···O H-bond CPs (Figure 8).

Table 8. Geometric features of experimental and computed Pt coordination.[a]

	BH&H	Exptl[b]
Pt–N1 [Å]	2.022	2.000
Pt–N2 [Å]	2.030	1.987
Pt–N7A [Å]	2.004	1.984
Pt–N7B [Å]	2.026	1.963
N7A-Pt-N1 [°]	85.9	91.2
N7A-Pt-N2 [°]	172.8	177.6
N7A-Pt-N7B [°]	89.2	87.4
N1-Pt-N2 [°]	95.2	91.2
N1-Pt-N7B [°]	170.4	178.5
N2-Pt-N7B [°]	88.3	90.2
Gua/Gua[c]	60.3	58.0

[a] See Figure 1a for labelling. [b] NMR data from Reedijk et al.[43] [c] See Orbell et al.[63] for convention of dihedral angles and Figure 1b.

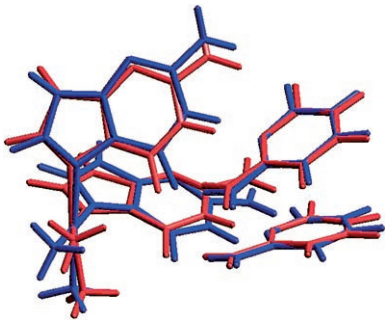

Figure 7. Overlay of optimised (red) and experimental (blue) platinated GpG·CpC.

The energetic consequences of this topology, and of differences between experimental and theoretical structures, are detailed in Table 9. Hydrogen bonds in the optimised structure contribute about 6–7 kcal mol^{-1} each to the stability of the complex, a similar figure to that found in model complexes. Stacking interactions between guanine residues is in both cases limited to a single interaction, corresponding to less than 2 kcal mol^{-1}, whereas stacking between cytosine residues is weaker than in smaller models, but slightly stronger in the optimised structure. Interstrand interactions are absent in the experimental structure and very weak in the optimised one. Although the effect on GC pairing follows the pattern established above, these effects are slightly more pronounced here than in smaller oligonucleotides: for instance H4···O6 bonds and H2···O2 are strongly perturbed by between 30 and 50%, but the overall H-bond energy is reduced by only about 2 kcal mol^{-1} from its original value.

One can envisage two main reasons for the observed differences between experimental and optimised geometries and electron densities. Firstly, NMR structures are by definition averaged over many conformations, whereas the optimised structure is a single static conformation that minimises the potential energy of the overall structure. It is perhaps

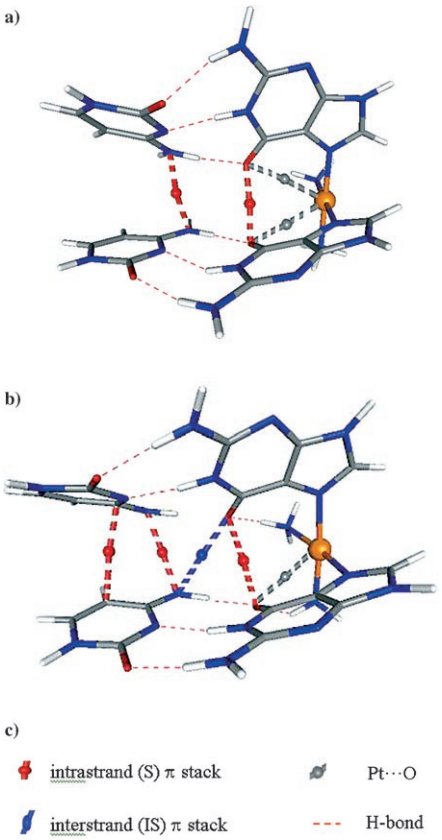

Figure 8. Representation of intermolecular interactions found in a) experimental and b) optimised geometry of platinated GpG·CpC from octamer complex.

Table 9. Intermolecular topology and energy in experimental and theoretical octamer structures.

	Exptl			BH&H		
	CPs	ρ_c	E	CPs	ρ_c	E
Pt–G	–	–	–	N–H···O	0.0309	7.65
				N–H···O	0.0210	5.90
GG_S	O···O	0.0107	1.87	O···O	0.0061	1.08
CC_S	N···N	0.0074	1.30	N···N	0.0101	2.87
				C···C	0.0064	
GC_{IS}	–	–	–	O···N	0.0071	1.23

not surprising, therefore, that more intermolecular contacts are seen in the optimised geometry, as they will certainly lead to reduction in energy where they are compatible with the demands of metal complexation and DNA backbone. Secondly, however, it is known[45] that while BH&H performs well for π-stacking interactions, it systematically overestimates the strength of hydrogen bonds. In the optimised structure (Figure 8), ammine ligands have rotated relative to guanine residues in order to maximise their hydrogen bonding to guanine O6, which may be due to shortcomings in the theoretical method or to differences between static and averaged conformations. Nonetheless, we stress that the performance of this approach is impressive given the difficulty of simultaneous modelling of platination, hydrogen bonding and π stacking.

Finally, throughout this work we have identified secondary interactions such as Pt···O and Pt···N by AIM analysis. Table 10 summarises all such interactions found and shows

Table 10. Secondary Pt···N(O) interactions in platinated oligonucleotides.

		Pt···X r [Å]	ρ [a.u.]
GpA_{mono}	Pt···N7	3.421	0.009
$GpGpG_{bi}$	Pt···O6	3.212	0.012
$GpGpG_{mono}$	Pt···N7	3.149	0.014
$GpG{\cdot}CpC_{bi}$	Pt···O6	3.026	0.017
$GpG{\cdot}CpC_{chel}$	Pt···N7	3.028	0.018
cis_{QM}	Pt···O6	3.042	0.017
cis_{exptl}	Pt···O6	3.311	0.010
	Pt···O6	3.412	0.008

that such contacts are always longer than 3 Å and rather weak, with ρ_c between 0.008 and 0.017 a.u., while no clear difference between Pt···O and Pt···N interactions is apparent. Thus, any contribution to the stability of complexes will be small, but they might exert some influence on geometry, since our data suggests that these interactions are directed to the axial positions about platinum: such weak axial interactions have been noted before.[31,76]

Conclusion

The combination of BH&H/6-311++G(d,p) and AIM analysis has allowed us to investigate the role of covalent and intermolecular forces in cisplatin–DNA adducts. Comparison with experimental geometries was found to be satisfactory for both cisplatin itself and its complexes with guanine. The interaction of cisplatin with single-strand DNA follows the pattern established experimentally, that is, complexes to guanine are more stable than those with adenine. Interactions of cisplatin's ammine and chloro ligands, which include N–H···Cl, Pt–N–H···O and Pt–N–H···N, dominate H-bond energies and contribute significantly to overall stabilisation. Both mono- and bifunctional complexation induces strong distortion: for instance, bifunctional cisplatin–DNA complexes show major disruption of π stacking between the bases bound to the metal. Complexes of cisplatin with DNA duplexes were also studied in order to monitor the effect of platination on both H-bonding and π stacking. Intramolecular H-bonds and covalent Pt–N bonds are close to those of single-stranded complexes, and the effect on the GC Watson–Crick pair is similar to that found in simple models such as platinated GC pair: the pattern of stabilisation is altered, but the overall stability of GC is virtually unchanged.

We have also presented data on a realistic model, namely, the platinated octamer cis[d(CCTG*G*TCC)·d(GGACCAGG)], for which NMR structural data is available. QM/MM calculations reproduced the experimental structure at the platinated GpG·CpC core: the RMS devia-

tion between calculated and optimised Cartesian coordinates is 2.12 Å, with bond lengths and angles within 0.06 Å and 8° of experimental values, respectively. AIM analysis shows that π-stacking interactions are seriously disrupted by platination, being reduced by more than 80% compared to unplatinated structures. The H-bonding pattern in the GC pair is affected in a similar manner as in smaller oligonucleotides, although the effect is more pronounced in the octamer structure. AIM reveals secondary Pt···O6 in both experimental and computed geometries; more studies are needed to clarify any biological relevance of such interactions.

[1] M. Gordon, S. Hollander, *J. Med.* **1993**, *24*, 209–265.
[2] R. B. Weiss, M. C. Christian, *Drugs* **1993**, *46*, 360–377.
[3] E. Wong, C. M. Giandomenico, *Chem. Rev.* **1999**, *99*, 2451–2466.
[4] M. D. Hall, T. W. Hambley, *Coord. Chem. Rev.* **2002**, *232*, 49–67.
[5] E. Cvitkovic, *Semin. Oncol.* **1998**, *25*, 1–3.
[6] J. Reedijk, *Chem. Commun.* **1996**, 801–806.
[7] A. Eastman, M. A. Barry, *Biochemistry* **1987**, *26*, 3303–3307.
[8] D. Lebwohl, R. Canetta, *Eur. J. Cancer* **1998**, *34*, 1522–1534.
[9] S. E. Sherman, S. J. Lippard, *Chem. Rev.* **1987**, *87*, 1153–1181.
[10] H. C. Harder, B. Rosenberg, *Int. J. Cancer* **1970**, *6*, 207–216.
[11] M. C. Lim, R. B. Martin, *J. Inorg. Nucl. Chem.* **1976**, *38*, 1911–1914.
[12] F. Basolo, H. B. Gray, R. G. Pearson, *J. Am. Chem. Soc.* **1960**, *82*, 4200–4203.
[13] H. B. Gray, R. J. Olcott, *Inorg. Chem.* **1962**, *1*, 481–485.
[14] H. M. Ushay, T. D. Tullius, S. J. Lippard, *Biochemistry* **1981**, *20*, 3744–3748.
[15] N. P. Johnson, J. D. Hoeschele, R. O. Rahn, *Chem. Biol. Interact.* **1980**, *30*, 151–169.
[16] P. Horacek, J. Drobnik, *Biochim. Biophys. Acta* **1971**, *254*, 341–347.
[17] M. Howegrant, K. C. Wu, W. R. Bauer, S. J. Lippard, *Biochemistry* **1976**, *15*, 4339–4346.
[18] J. Kozelka, F. Legendre, F. Reeder, J. C. Chottard, *Coord. Chem. Rev.* **1999**, *192*, 61–82.
[19] P. Mills, C. F. Anderson, M. T. Record, *J. Phys. Chem.* **1985**, *89*, 3984–3994.
[20] J. L. Jestin, B. Lambert, J. C. Chottard, *J. Biol. Inorg. Chem.* **1998**, *3*, 515–519.
[21] P. M. Takahara, A. C. Rosenzweig, C. A. Frederick, S. J. Lippard, *Nature* **1995**, *377*, 649–652.
[22] C. J. Van Garderen, L. P. A. Van Houte, *Eur. J. Biochem.* **1994**, *225*, 1169–1179.
[23] F. Aprile, D. S. Martin, *Inorg. Chem.* **1962**, *1*, 551–557.
[24] J. W. Reishus, D. S. Martin, *J. Am. Chem. Soc.* **1961**, *83*, 2457–2462.
[25] M. Kruidering, B. van de Water, Y. Zhan, J. J. Baelde, E. de Heer, G. J. Mulder, J. L. Stevens, J. F. Nagelkerke, *Cell Death Differ.* **1998**, *5*, 601–614.
[26] V. M. Gonzalez, M. A. Fuertes, C. Alonso, J. M. Perez, *Mol. Pharmacol.* **2001**, *59*, 657–663.
[27] K. Spiegel, P. Carloni, U. Rothlisberger, *J. Phys. Chem. B* **2004**, *108*, 2699–2707.
[28] E. Tornaghi, W. Andreoni, P. Carloni, J. Hutter, M. Parrinello, *Chem. Phys. Lett.* **1995**, *246*, 469–474.
[29] P. N. V. Pavankumar, P. Seetharamulu, S. Yao, J. D. Saxe, D. G. Reddy, F. H. Hausheer, *J. Comput. Chem.* **1999**, *20*, 365–382.
[30] Y. Zhang, Z. Guo, X. Z. You, *J. Am. Chem. Soc.* **2001**, *123*, 9378–9387.
[31] A. Robertazzi, J. A. Platts, *J. Comput. Chem.* **2004**, *25*, 1060–1067.
[32] J. V. Burda, J. Leszczynski, *Inorg. Chem.* **2003**, *42*, 7162–7172.
[33] M. H. Baik, R. A. Friesner, S. J. Lippard, *J. Am. Chem. Soc.* **2003**, *125*, 14082–14092.
[34] R. K. O. Sigel, B. Lippert, *Chem. Commun.* **1999**, 2167–2168.
[35] J. V. Burda, J. Sponer, J. Leszczynski, *Phys. Chem. Chem. Phys.* **2001**, *3*, 4404–4411.
[36] R. K. O. Sigel, E. Freisinger, B. Lippert, *J. Biol. Inorg. Chem.* **2000**, *5*, 287–299.
[37] J. Raber, C. B. Zhu, L. A. Eriksson, *J. Phys. Chem. B* **2005**, *109*, 11006–11015.
[38] M. Zeizinger, J. V. Burda, J. Leszczynski, *Phys. Chem. Chem. Phys.* **2004**, *6*, 3585–3590.
[39] P. Carloni, M. Sprik, W. Andreoni, *J. Phys. Chem. B* **2000**, *104*, 823–835.
[40] A. Robertazzi, J. A. Platts, *Inorg. Chem.* **2005**, *44*, 267–274.
[41] A. Robertazzi, J. A. Platts, *J. Phys. Chem. A* **2006**, *110*, 3992–4000.
[42] A. D. Becke, *J. Chem. Phys.* **1993**, *98*, 1372–1377.
[43] D. Z. Yang, S. Vanboom, J. Reedijk, J. H. Vanboom, A. H. J. Wang, *Biochemistry* **1995**, *34*, 12912–12920.
[44] Gaussian 03, Revision B.05, M. J. Frisch, G. W. Trucks, H. B. Schlegel, G. E. Scuseria, M. A. Robb, J. R. Cheeseman, J. A. Montgomery, Jr., T. Vreven, K. N. Kudin, J. C. Burant, J. M. Millam, S. S. Iyengar, J. Tomasi, V. Barone, B. Mennucci, M. Cossi, G. Scalmani, N. Rega, G. A. Petersson, H. Nakatsuji, M. Hada, M. Ehara, K. Toyota, R. Fukuda, J. Hasegawa, M. Ishida, T. Nakajima, Y. Honda, O. Kitao, H. Nakai, M. Klene, X. Li, J. E. Knox, H. P. Hratchian, J. B. Cross, C. Adamo, J. Jaramillo, R. Gomperts, R. E. Stratmann, O. Yazyev, A. J. Austin, R. Cammi, C. Pomelli, J. W. Ochterski, P. Y. Ayala, K. Morokuma, G. A. Voth, P. Salvador, J. J. Dannenberg, V. G. Zakrzewski, S. Dapprich, A. D. Daniels, M. C. Strain, O. Farkas, D. K. Malick, A. D. Rabuck, K. Raghavachari, J. B. Foresman, J. V. Ortiz, Q. Cui, A. G. Baboul, S. Clifford, J. Cioslowski, B. B. Stefanov, G. Liu, A. Liashenko, P. Piskorz, I. Komaromi, R. L. Martin, D. J. Fox, T. Keith, Al-M. A. Laham, C. Y. Peng, A. Nanayakkara, M. Challacombe, P. M. W. Gill, B. Johnson, W. Chen, M. W. Wong, C. Gonzalez,, J. A. Pople, Gaussian, Inc., Pittsburgh, PA, **2003**.
[45] M. P. Waller, A. Robertazzi, J. A. Platts, D. E. Hibbs, P. A. Williams, *J. Comput. Chem.* **2006**, *27*, 491–504.
[46] F. Maseras, K. Morokuma, *J. Comput. Chem.* **1995**, *16*, 1170–1179.
[47] T. Matsubara, S. Sieber, K. Morokuma, *Int. J. Quantum Chem.* **1996**, *60*, 1101–1109.
[48] M. Svensson, S. Humbel, R. D. J. Froese, T. Matsubara, S. Sieber, K. Morokuma, *J. Phys. Chem.* **1996**, *100*, 19357–19363.
[49] M. Svensson, S. Humbel, K. Morokuma, *J. Chem. Phys.* **1996**, *105*, 3654–3661.
[50] S. Humbel, S. Sieber, K. Morokuma, *J. Chem. Phys.* **1996**, *105*, 1959–1967.
[51] D. Andrae, U. Haussermann, M. Dolg, H. Stoll, H. Preuss, *Theor. Chim. Acta* **1990**, *77*, 123–141.
[52] W. D. Cornell, P. Cieplak, C. I. Bayly, I. R. Gould, K. M. Merz, D. M. Ferguson, D. C. Spellmeyer, T. Fox, J. W. Caldwell, P. A. Kollman, *J. Am. Chem. Soc.* **1995**, *117*, 5179–5197.
[53] R. F. W. Bader, *Atoms in Molecules—A Quantum Theory*, Oxford, University Press, Oxford, **1990**.
[54] P. L. A. Popelier, *Atoms in Molecules: An Introduction*, Prentice Hall, Harlow, **2000**.
[55] J. Biegler-König, J. Schönbohm, *J. Comput. Chem.* **2002**, *23*, 1489–1494.
[56] R. F. W. Bader, H. Essen, *J. Chem. Phys.* **1984**, *80*, 1943–1960.
[57] S. J. Grabowski, *Chem. Phys. Lett.* **2001**, *338*, 361–366.
[58] E. Espinosa, M. Souhassou, H. Lachekar, C. Lecomte, *Acta Crystallogr. Sect. B* **1999**, *55*, 563–572.
[59] S. F. Boys, F. Bernardi, *Mol. Phys.* **1970**, *19*, 553.
[60] G. H. W. Milburn, M. R. Truter, *J. Chem. Soc. A* **1966**, 1609.
[61] P. Carloni, W. Andreoni, J. Hutter, A. Curioni, P. Giannozzi, M. Parrinello, *Chem. Phys. Lett.* **1995**, *234*, 50–56.
[62] S. E. Sherman, D. Gibson, A. H. J. Wang, S. J. Lippard, *J. Am. Chem. Soc.* **1988**, *110*, 7368–7381.
[63] J. D. Orbell, L. G. Marzilli, T. J. Kistenmacher, *J. Am. Chem. Soc.* **1981**, *103*, 5126–5133.
[64] A. Eastman, *Biochemistry* **1986**, *25*, 3912–3915.
[65] A. M. J. Fichtingerschepman, J. L. Vanderveer, J. H. J. Denhartog, P. H. M. Lohman, J. Reedijk, *Biochemistry* **1985**, *24*, 707–713.

[66] M. S. Davies, S. J. Berners-Price, T. W. Hambley, *J. Am. Chem. Soc.* **1998**, *120*, 11380–11390.
[67] I. L. Zilberberg, V. I. Avdeev, G. M. Zhidomirov, *J. Mol. Struct.* **1997**, *418*, 73–81.
[68] A. Pelmenschikov, I. Zilberberg, J. Leszczynski, A. Famulari, M. Sironi, M. Raimondi, *Chem. Phys. Lett.* **1999**, *314*, 496–500.
[69] G. L. Cohen, W. R. Bauer, J. K. Barton, S. J. Lippard, *Science* **1979**, *203*, 1014–1016.
[70] M. Sip, A. Schwartz, F. Vovelle, M. Ptak, M. Leng, *Biochemistry* **1992**, *31*, 2508–2513.
[71] F. Herman, J. Kozelka, V. Stoven, E. Guittet, J. P. Girault, T. Huynh-dinh, J. Igolen, J. Y. Lallemand, J. C. Chottard, *Eur. J. Biochem.* **1990**, *194*, 119–133.
[72] J. A. Rice, D. M. Crothers, A. L. Pinto, S. J. Lippard, *Proc. Natl. Acad. Sci. USA* **1988**, *85*, 4158–4161.
[73] J. H. J. Denhartog, C. Altona, J. H. Vanboom, G. A. Vandermarel, C. A. G. Haasnoot, J. Reedijk, *J. Biomol. Struct. Dyn.* **1985**, *2*, 1137–1155.
[74] J. H. J. Denhartog, C. Altona, G. A. Vandermarel, J. Reedijk, *Eur. J. Biochem.* **1985**, *147*, 371–379.
[75] M. Orozco, A. Perez, A. Noy, F. J. Luque, *Chem. Soc. Rev.* **2003**, *32*, 350–364.
[76] a) J. Kozelka, J. Bergès, R. Attias, J. Freitag, *Angew. Chem.* **2000**, *112*, 204–207; *Angew. Chem. Int. Ed.* **2000**, *39*, 198–201.

Received: December 14, 2005
Published online: May 19, 2006

